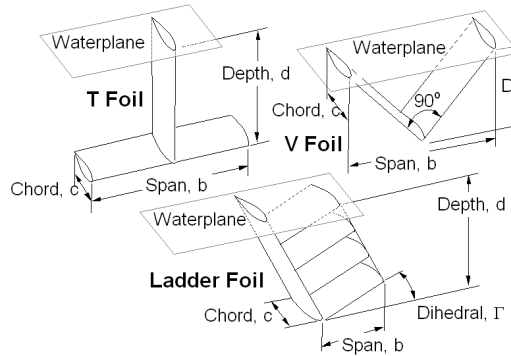


## APPENDIX B: GENERIC HYDROFOIL TRADE STUDY

Perhaps the most important consideration after the system requirements is the type of hydrofoil to employ. Three generic types of hydrofoil were considered: fully submerged inverted "T" foils, and surface piercing "V" foils and ladder foils. These are shown schematically in Figure B1. The purpose of this study was not to produce a finished design, but to simply explore the relative merits of the three types of hydrofoil and to establish some approximate operating parameters. Actual design analyses will be done with more sophisticated methods.



**Fig B1** Generic Hydrofoil Types

The fully submerged T foil is insensitive to depth of submergence, and therefore must be equipped with some sort of feedback control system to measure the craft's height above water and alter the lift on the hydrofoil, either through changing the foil's incidence or a trailing edge flap, so as to maintain the desired flying height. The heave stiffness of such a system is totally dependent upon the loop gain in the feedback system.

The surface piercing foils are fixed, but change their underwater geometry as a function of the boat's heave, pitch and roll. Ideally, the boat stays level, maintaining the same angle of attack and the foils reach equilibrium by adjusting their area with little change in lift coefficient. The heave stiffness of such a system is a function of its geometry and cannot be specified independent of the foil's performance requirements.

### Methodology

For this rough analysis, the three types of hydrofoils were compared using handbook methods (Hoerner, 1965). All foils were evaluated with a load of 3500 lb, representing 50% of the design weight. The aspect ratio of all three types was set at 6. The aspect ratio of

a real design would depend strongly on structural considerations. The surface piercing foils were assumed to operate with the craft's pitch attitude held level, thus maintaining a constant angle of attack and an approximately constant lift coefficient.

The T foil was assumed to operate at a depth of three chord-lengths. The T foil was optimized for a speed of 15 kt, as a compromise between low and high speed drag.

The V-foil was assumed to have an interior angle of 90 degrees, which resulted in its depth being one-half the span. The V foil was optimized to minimize its drag at 12 kt.

The ladder foil's height was determined by the span and its dihedral angle. The spacing of the rungs was set such that at the given dihedral opposite ends of successive rungs were at the same height, giving a constant variation in the area with depth of submergence. The selected dihedral, 20 degrees, resulted in a rung spacing of approximately two chord-lengths. The ladder foil was further constrained to have three rungs submerged at 12 kt. The ladder foil was also optimized to minimize its drag at 12 kt.

$$B1) \quad D = q \cdot C_f \cdot S_w + q \cdot N_j \cdot C_{Dj} \cdot t^2 + q \cdot N_s \cdot C_{Ds} \cdot t^2 \dots \\ + S \cdot q \cdot C_{Dw} + \frac{1}{q} \cdot \frac{L^2}{\left[ \pi \cdot (b^2 \cdot E) \right]}$$

$$B2) \quad C_{Dw} = \frac{1}{2} \cdot k_w \cdot \frac{L^2}{(b^2 \cdot d \cdot q^2 \cdot V^2)} \cdot g$$

$$B3) \quad q = \frac{1}{2} \cdot \rho \cdot V^2$$

The basic drag equation was:

The first term represents the drag due to viscous effects. Since the profile drag of the candidate sections was approximately 0.006 and varied little with angle of attack, the wetted area was taken as twice the planform area for a given element and the skin friction drag coefficient,  $C_f$ , was set to 0.003. Strictly speaking, this included pressure (form) drag with the skin friction, but it made it possible to account for the increased wetted area due to dihedral and struts.

The second term is the interference drag at the junctions.  $N_j$  is the number of 90 degree junctions,  $t$  is the foil thickness (in feet) and the drag coefficient,  $C_{Dj}$ , was taken as 0.1, which is half the value for a complete T junction as reported by Hoerner.  $N_j$  was 2 for the T foil and 1 for the V foil. For the ladder foil, it varied with depth according to the relationship:

$$B4) N_j = 4 \cdot N_r - 3$$

Where  $N_r$  is the number of rungs in the water.  $N_j$  and  $N_r$  were allowed to take on real values so as to represent an averaged value and avoid jumps in the drag as depth changed.  $N_r$  was also constrained to equal three at 12 kt.

The third term is the spray drag. Hoerner gives a value of 0.24 for the drag coefficient,  $C_{Ds}$ , for an upright streamlined strut, and this was used for both struts and lifting foil elements, regardless of the angle at which they left the water. The number of elements leaving the water,  $N_s$ , was taken as one for the T foil, two for the V foil and 3 for the ladder foil.

The next term, wave drag,  $C_{Dw}$ , turned out to be so small as to be negligible because all of the cases were run at high Froude numbers based on the hydrofoil chord.

The final term was the induced drag due to the lift on the hydrofoil. The efficiency factor,  $E$ , was taken to be 0.98 for the T foil. Experimental data in (Hoerner, 1965) suggest a value of 0.64 for the 90 degree V foil. The efficiency of the ladder foil is ideally double that of the T foil because of the end-plate effect of the struts which turn it into a boxplane configuration. However, the ladder foil also has rungs operating closer to the surface. At the surface, the induced drag is doubled. So the data in (Hoerner, 1965) were curve fit as a function of the average depth, and  $E$  ranged from 0.62 to 1.92 for the depths investigated. No account was made for the interference effects of one rung on another, and no credit was taken for the increase in physical span due to the inclination of the struts and the resultant lateral stagger of the rungs.

The major difference between the configurations was the manner in which the lift coefficient, area, depth and span varied with speed. The T foil was assumed to run at constant depth and its lift coefficient varied with speed:

$$B5) C_L = 2 \cdot \frac{W}{(S \cdot \rho \cdot V^2)}$$

The V foil was assumed to operate at a constant lift coefficient. Its planform area and wetted area varied as:

$$B6) S = 2 \cdot \frac{W}{(C_L \cdot \rho \cdot V^2)}$$

$$B7) S_w = 2 \cdot \sqrt{2} \cdot S$$

$$B8) c = \frac{b_{\text{takeoff}}}{A} = \sqrt{\frac{S_{\text{takeoff}}}{A}}$$

$$B9) h = \frac{b}{2} = \frac{S}{2 \cdot c}$$

Two variations of the V foil were investigated. The first was a constant chord foil, and all of the parameters were as given above. The second variation was a tapered foil, with triangular panels joined at their apex. For this variation the number of junctions was effectively zero and the induced drag efficiency,  $E$ , was lowered to 0.4 to reflect the poor spanwise lift distribution resulting from the reduction to zero at the center.

The relationships for the ladder foil were more complex. Lift coefficient was assumed constant. The total area was taken as the sum of the planform areas of the rungs. The number of rungs varied with depth and thus the total area in the same manner as for the V foil (equation 28). The span was constant until the last rung was reached, at which point it shrank with decreasing depth. The principal difference between this foil's behavior and the constant chord V foil was that the span did not reduce so quickly as depth was adjusted to match the required area.

$$B10) N_r = S \cdot \frac{A}{b^2}$$

$$B11) d = N_r \cdot b \cdot \sin(\Gamma) \cdot \cos(\Gamma)$$

$$B12) S_{\text{wet}} = 2 \cdot c \cdot b \cdot \left[ \sin(\Gamma) \cdot (N_r + \max(N_r - 1, 0)) \dots + N_r \cdot \cos(\Gamma) \right]$$

With this modeling in place, the drag could be calculated at any speed, and the parameters varied to minimize the drag at the design condition. The resulting foil dimensions at 12 kt are shown in Figure B2. The V foil has the greatest span at 12 feet and the ladder foil the least at 7 feet. Lift coefficient for the T foil was 0.71 at 12 kt and 0.46 at 15 kt, 0.36 for the constant chord V foil, 0.27 for the tapered V foil, and

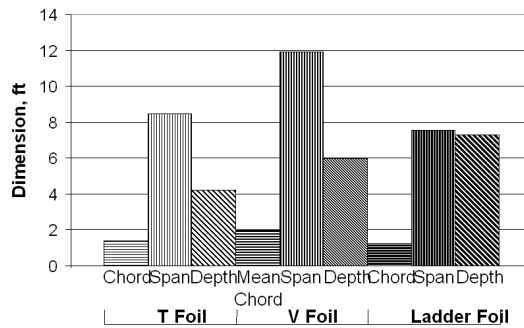
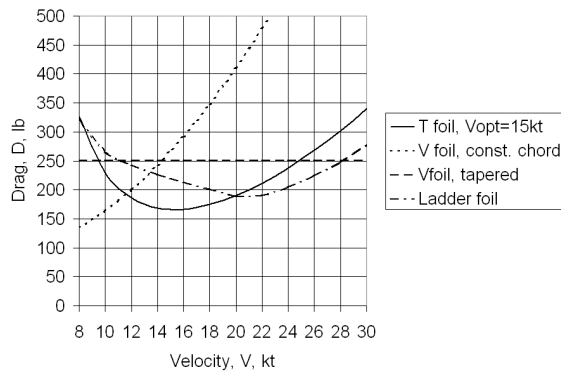


Fig. B2, Generic Hydrofoil Dimensions

0.30 for the ladder foil. These are all reasonable values, based on the H105 section design.

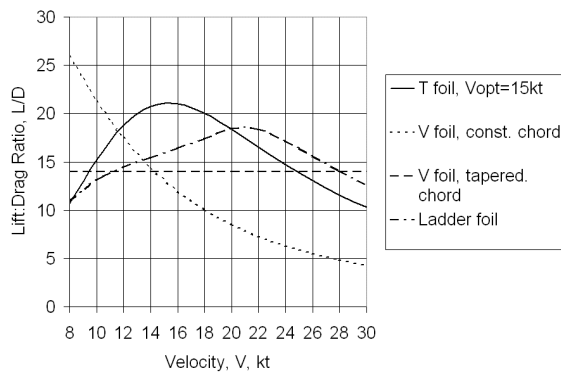
### Results

Figure B3 shows the drag calculated for all four foils. As expected, the T foil had the lowest drag. However, it suffered at speeds well away from its design condition. The constant chord V foil was the worst, with a steeply rising drag curve. However, the tapered V foil had the remarkable characteristic of constant drag, independent of speed. The ladder foil had an almost V-shaped drag curve, wider and shallower than the T foil with 20% more drag at 12 kt. From 20 kt to 30 kt, the ladder foil was predicted to have the least drag. Under these conditions, it is virtually a V foil, since only the last rung is in the water.



**Fig. B3, Generic Hydrofoil Drag**  
W = 3500 lb, A = 6

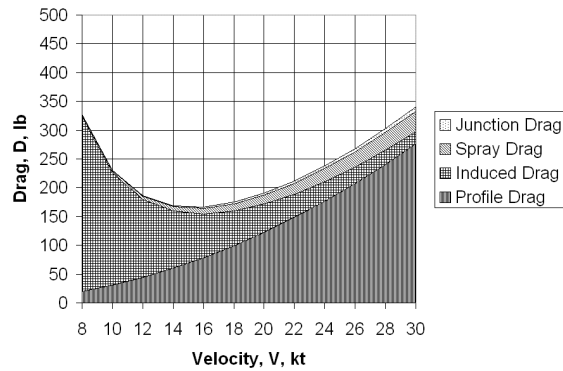
Lift/drag ratios (Figure B4) for all the foils except the constant chord V foil exceed 12 over a twenty-knot range, with the T foil peaking out at an L/D of 21. The constant chord V foil will not meet the requirements.



**Fig. B4, Generic Hydrofoil L/D**  
W = 3500 lb, A = 6

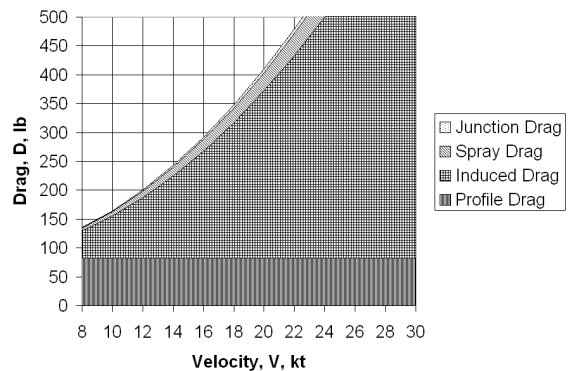
Figure B5 shows the breakdown of the T foil drag into its components. The junction and spray drags are minor. The drag is dominated by the induced drag at low speed and the parasite drag (skin friction plus form,

spray, and interference drags) at high speed. The induced drag drops as velocity squared, the parasite drag increases as velocity squared, and at the speed for minimum drag and maximum L/D the induced drag equals the parasite drags. This is the basic characteristic of aircraft performance, too, and stems from the fixed span and fixed area.



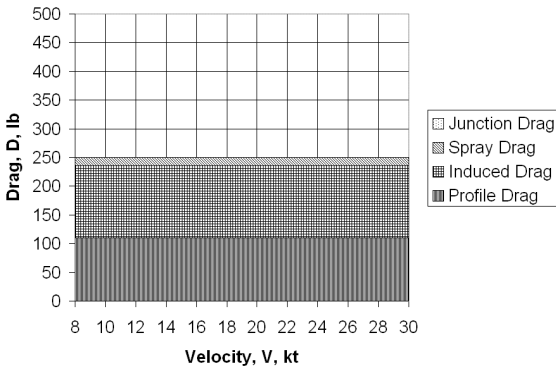
**Fig. B5, Generic T Foil Drag Breakdown**  
W = 3500 lb, A = 6

Figure B6 shows the breakdown of the constant chord V foil drag components. The profile drag is seen to be constant and independent of speed. This is a result of the assumption of constant lift coefficient. The profile drag per unit area is increasing with speed squared, but the area is decreasing with speed squared and the two trends cancel. The induced drag is increasing rapidly with speed however. This is a result of the span shrinking with speed squared in order to maintain the required area. Since the induced drag depends on span squared, this produces a velocity to the fourth power dependence which is only partially canceled by the dynamic pressure term. The shrinking aspect ratio of the V foil would appear to create a barrier to high speeds unless the aspect ratio can be made exceptionally high or the angle of attack changed with speed so as to reduce the lift and immerse more of the foil.



**Fig. B6, Generic V Foil Drag Breakdown**  
Constant Chord, W = 3500 lb, A = 6

In contrast to the constant chord V foil, the tapered chord V foil's induced drag does not suffer so badly with speed. (Figure B7). Its span drops with the square root of speed, since both the span and the chord are shrinking at the same time. The result is that the span dependence and the speed dependence of the induced drag cancel, and the induced drag is independent of speed. Likewise, the thickness also goes down with speed, so the spray drag is also speed independent. The paradoxical result is a hydrofoil whose drag is constant. A more sophisticated analysis would have to be performed to properly set the level of the induced drag and spray drags due to the large chord at the surface.



**Fig. B7,** Generic V Foil Drag Breakdown  
Tapered Chord,  $W = 3500$  lb,  $A = 6$

The ladder foil's drag makeup has elements that are similar to both the V foil and the T foil (Figure B8). Like the V foils, the profile drag at low and medium speeds is constant. Owing to its fixed span, the induced drag decreases with speed like the T foil. Once the last rung is reached, the induced drag begins to increase rapidly like the constant chord V foil. This is partially balanced by a reduction in profile drag due to the reduced wetted area of the strut. The level of the profile drag at low speeds is higher than the other foils because of the extra wetted surface of the struts.

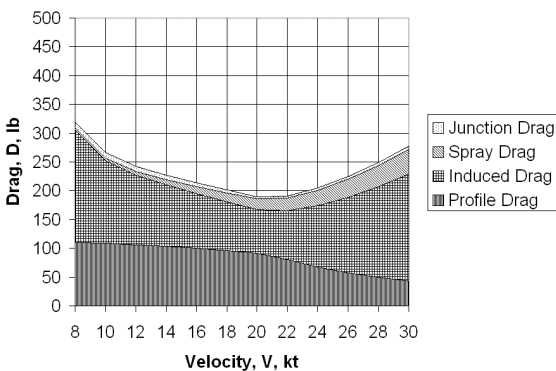


**Fig. B8,** Generic Ladder Foil Drag Breakdown  
 $W = 3500$  lb,  $A = 6$

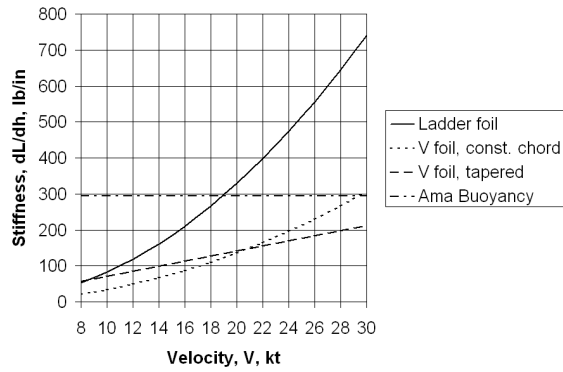


**Fig. B9,** Generic Hydrofoil Heave Stiffness  
 $W = 3500$  lb,  $A = 6$

The final comparison of the generic foil types is their heave stiffness (Figure B9). Also shown for reference is the heave stiffness of the ama at a comparable loading. The T foil is not shown because its stiffness depends on a feedback control system and is therefore arbitrary. The V foils provide less stiffness than that from buoyancy over the entire speed range. They are extremely soft at low speeds. If used for the lateral foil, this may not provide sufficient stability. The ladder foil has considerably more stiffness and may be excessively stiff at speeds much above 20 kt. However, this stiffness may be required for stability.

### Comparison with Test Data

The methodology of the generic hydrofoil trade study was validated by comparison with test data. These results are presented in Appendix C, and included Bell's HD-4 equipped with ladder foils and a configuration with both a constant chord V foil and an inverted T foil.

None of the tests reported included all the information necessary to predict the results. However, in general, it was possible to match the test data with a reasonable selection of parameter values. The variation of drag with speed was matched very well.

The behavior of the V foil was qualitatively similar to the inverted T foil for some of the data, and like the generic V foil prediction for other portions of the data. The difference was due to the powerful influence of the aft T foil on the craft's pitch trim. This demonstrates that it is essential to take into account the whole configuration and the results from examining a hydrofoil unit in isolation are highly dependent upon the initial assumptions as to how the unit is operated.

In conclusion, the generic model is capable of showing the variation in hydrofoil drag with speed, however it is best applied to the whole configuration of the craft rather than to isolated foil units.

## APPENDIX C: TEST DATA COMPARISONS

### Bell HD-4

The methodology for the generic ladder foil study was applied to data from the HD-4, a ladder-type hydrofoil invented by Alexander Graham Bell and tested in 1917. The HD-4 was a trimaran, 60 feet long, 20 feet in beam, and weighed 10,400 lb. It sustained a speed of over 46 kt on its welded steel hydrofoils (Baldwin, 1917). A general arrangement of the craft is shown in Figure C1.

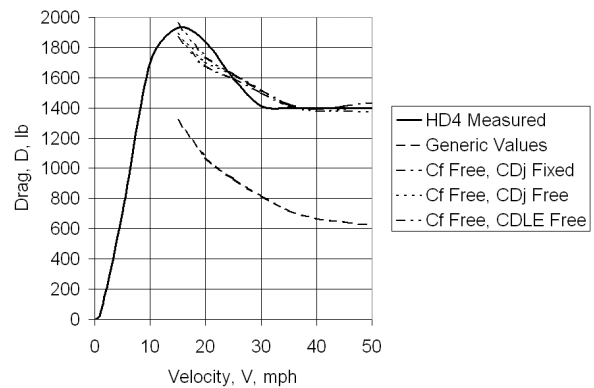
For the analysis, each main and stern foil was modeled separately. Model parameters were optimized to a least squares fit of the test data from 20 kt to 50 kt. Based on photographs of the craft running, the bow foil is completely out of the water, and the craft has a pitch attitude of approximately two degrees. Baldwin reports that at 50 kt the craft was planing with a foil loading of 1486 psf, which corresponds to a lift coefficient of 0.27. This implies a fully submerged lift coefficient of 0.54, and therefore this value was used for the main foils. Lift coefficient for the stern foil was set at 0.088, which gave a pitch attitude at speed of 1.8 degrees. The main foils were set at an incidence of 5.5 degrees, and the difference in lift coefficients is consistent with this. The number of rungs showing above the water was also consistent with the photographs.

The HD-4 used a sharp-edged section, and this could experience separation and added drag when the angle of attack was greater than the ideal angle. The improvement in L/D for the HD-4 as the main foil incidence was reduced was consistent with this behavior. So an additional parasite drag term,  $C_{DLE}$ , proportional to the total planform area, was added to the model to investigate this effect.

Parameter	Generic	Free Parameter		
		$C_f$	$C_f$ & $C_{Dj}$	$C_f$ & $C_{DLE}$
$C_f$	0.003	0.0089	0.0087	0.0061
$CD_j$	0.100	0.0100	0.199	0.100
$CD_{LE}$	0.000	0.0000	0.000	0.0090

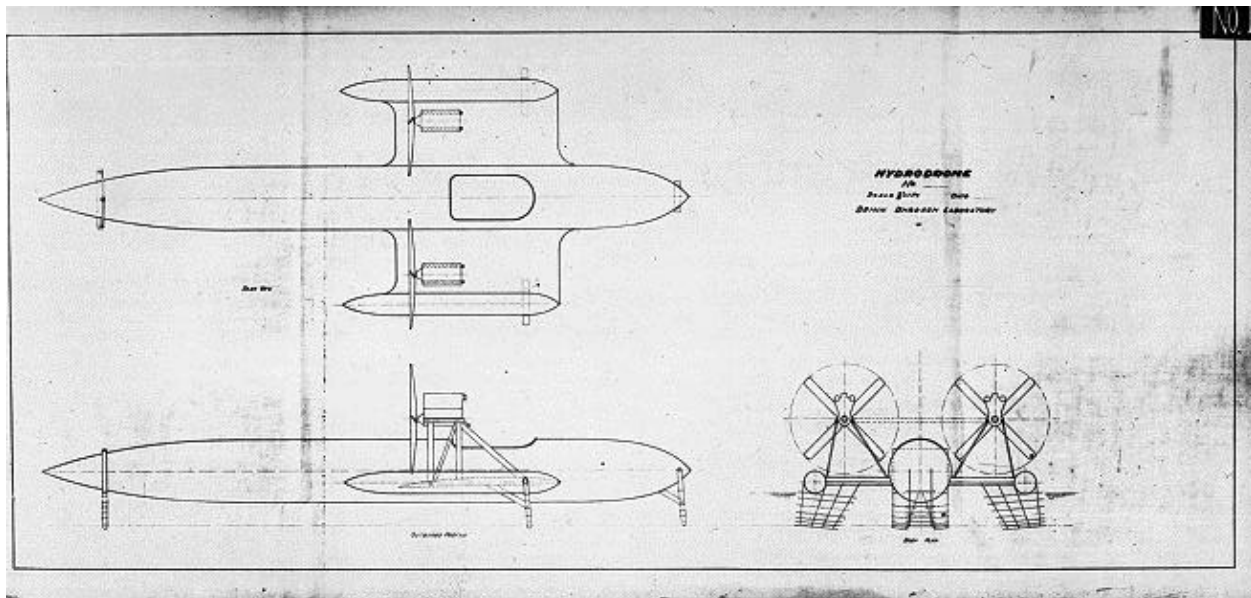
**Table C1** Model Matching Parameters

Four variations of the model parameters were used. The first variation had the same parameters as used in the generic analysis. The second variation allowed the skin friction coefficient to vary. The third varied both the skin friction and junction drag coefficients, and the last varied the skin friction and leading edge drag coefficients. Table 1 shows the fitted values of the model parameters.



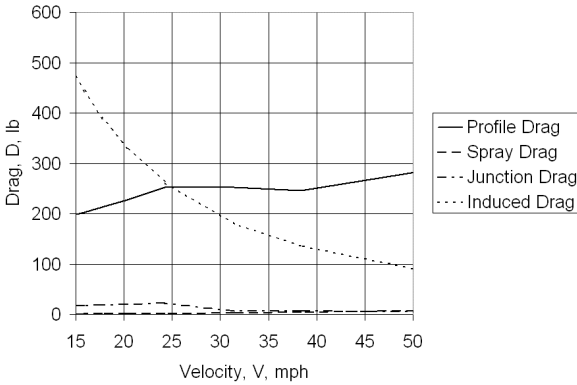
**Fig. C2** Model Drag vs. HD-4 Test Data

Figure C2 shows the comparison of the predicted drag with the test data. The generic values were considerably in error. Allowing the profile drag/skin friction to vary resolved most of the difference, and



**Fig. C1** Bell HD-4 General Arrangement

only a small improvement was obtained with the other parameters. The best fit was with the leading edge drag, and the fitted value is about half the additional drag due to a sharp leading edge as reported by Hoerner. The remaining higher skin friction drag can be attributed to the turbulent sections used on the HD4's struts and foils compared to the laminar flow sections assumed in the generic analysis. The doubling of the junction drag did not make a significant difference in the fit of the model to the data, as seen in Figure C3.



**Fig. C3** HD-4 Main Foil Drag

### Smits V Foil Tow Tank Results

The ladder and T foil methodology was validated by comparison with tow tank data from (Smits and Verkerk, 1981). The configuration consisted of a 1/3 scale Flying Dutchman dinghy equipped with a large V foil forward and an inverted T foil rudder. The model was tested as a graduate student project at Delft University under the direction of Prof. J. Gerritsma.

The geometry of the model is shown in Figure C4. Several variations in the model were tested, with the geometric parameters for the first four test series given in Table C2.

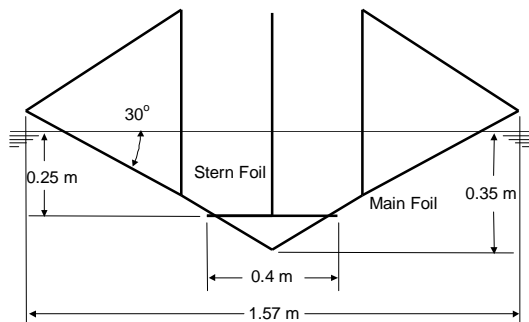


**Fig. C4**, Tow Tank Model Foil Geometry

Series	V foil depth	V foil angle	T foil depth	T foil span	T foil angle
1	0.35 m	3 deg	0.25 m	0.4 m	3 deg
2	0.29 m	3 deg	0.19 m	0.4 m	3 deg
3	0.29 m	3 deg	0.19 m	0.3 m	3 deg
4	0.29 m	3 deg	0.19 m	0.3 m	1.5 deg

**Table C2** Tow Tank Model Parameters

The hydrodynamic model parameters are presented in Table C3. A modest increase in the profile drag to account for the sharp leading edge improved the fit to the data at high speeds, but the generic value did a good job of matching the data. The drag of the foil junction was set to one-half that of a 90 degree junction to represent the 120 degree interior angle of the model configuration. The induced drag efficiency factor, E, was calculated to be 0.7 for the V foil, based on a lifting line analysis (Speer, 2000). Since the T foil tended to ride very close to the surface, its value of E was taken to be 0.5. The angle of zero lift for the 6% thick circular arc sections was assumed to be -3 degrees and the two-dimensional lift coefficient slope,  $a_0$ , was assumed to be 0.11 per degree of angle of attack. The load carried by the main foil was reported to be 84N and the load carried by the stern foil was 42N.

Parameter	Generic	V foil	T foil	alpha0
Cf	0.003	0.004	0.004	-3 deg
CDj	0.10	0.05	0.10	-3 deg
CDs	0.24	0.24	0.24	-3 deg
E	0.67	0.70	0.50	-3 deg

**Table C3** Model Matching Parameters

The prediction of trim angle of attack was critical to predicting the variation in lift and drag with speed. The three-dimensional lift curve was calculated according to

$$C1) \quad C_L = \frac{a_0}{1 + \frac{180}{\pi} \cdot \frac{a_0}{\pi \cdot A \cdot E}} \cdot \alpha$$

Where the angle of attack,  $\alpha$ , is taken relative to the zero lift line, which for this section was three degrees greater than the pitch attitude.

Since the area of the stern foil did not change, its angle of attack was found by solving equation C1 for angle of attack. The immersed span of the V foil was found using a more sophisticated formula than for the generic analysis that took into account the change in the lift due to both area and angle of attack:

$$C2) b = \frac{1}{(2 \cdot \pi)} \cdot \frac{\left[ W \cdot \pi \cdot E + \sqrt{W \cdot E \cdot \left( W \cdot \pi^2 \cdot E + 720 a_0^2 \cdot \alpha \cdot q \cdot c^2 \right)} \right]}{\left( a_0 \cdot E \cdot \alpha \cdot q \cdot c \right)}$$

The test model included both hull and hydrofoils, therefore it was not possible to properly estimate the lift and drag when the hull was in the water. Test observers reported that the main foil lifted first, and the stern had a tendency to drag until the T foil lifted it out of the water. So an arbitrary limit was placed on the pitch attitude of six degrees. When the pitch attitude was less than six degrees, the boat was assumed to be fully foil borne, and when the pitch attitude was on the limit, it was assumed to be restrained by the hull buoyancy. Only the predictions for fully foilborne operation are presented.

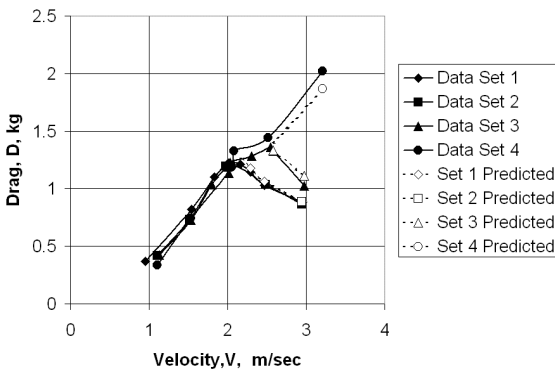


**Fig. C5, Tank Test Drag Comparison**

The resulting match between the test data and the analytical model is shown in Figures C5 and C6. The model fits the data very well.

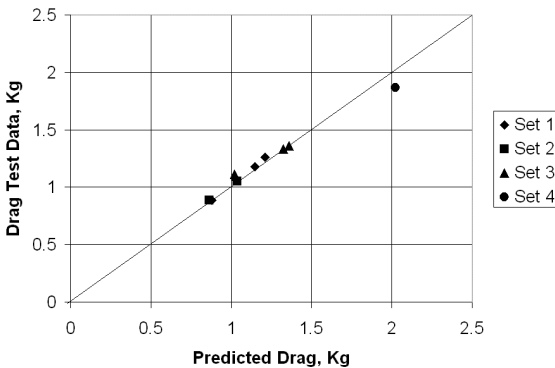


**Fig. C6, Tank Test Data vs. Prediction**

The predicted pitch attitude is shown in Figure C7. The difference in the drag behavior between Series 3 and Series 4 is due to the change in incidence of the T foil. The increased angle of attack resulted in the stern foil being constrained to ride at the surface, and the

pitch attitude increased with speed as the V foil rose higher out of the water. This exaggerated the reduction in span and raised the induced drag compared with the generic hydrofoil trade study.

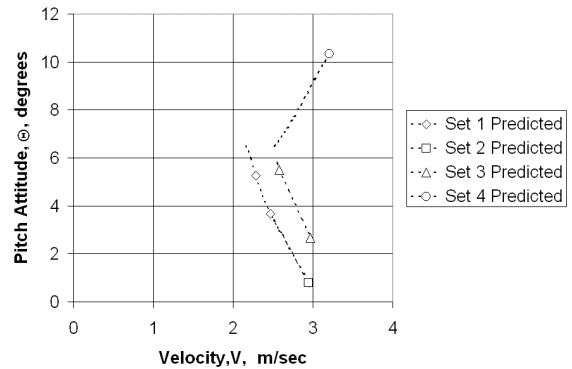


**Fig. C7, Predicted Pitch Attitude**

These results demonstrate the critical role played by the pitch trim of the craft and the interaction between the forward and aft hydrofoils. The results of the generic study for the constant chord V foil are seen to be a reflection of the initial assumptions, such as constant lift coefficient, as much as an indication of the behavior of a class of hydrofoils.

This suggests an organized approach to the design of a surface piercing hydrofoil configuration consisting of the following steps:

- 1) Estimate the load carried by each foil based on the external loads applied to the craft.
- 2) Design the main foil(s) to meet the performance requirements.
- 3) Determine the optimum angle of attack for operating the main foil as a function of speed.
- 4) Tailor the design of the stern foil to optimize the performance of the craft. For pitch stability, the aft foil should be more lightly loaded than the main foils and the relative change in lift with heave should be less than the main foil. The variation in stern foil lift with heave should be set so as to balance the boat at the angle of attack required for best performance of the main foils.
- 5) Provide some means for adjusting the incidence of the stern foil. Given the effect of stern foil incidence on the trim of the craft, it may not be necessary to change the incidence of the main foil(s). But some means of tuning for performance should be provided.